Study of the Low-Lying States of Cl^{38} via the Reaction $Cl^{37}(d, p\gamma)Cl^{38}$ †

G. A. P. Engelbertink and J. W. Olness
Physics Department, Brookhaven National Laboratory, Upton, New York 11973
(Received 6 August 1971)

Levels of Cl^{38} below an excitation energy of 2.75 MeV have been studied with the reaction $Cl^{37}(d,p\gamma)Cl^{38}$ at a deuteron bombarding energy of 3.1 MeV. γ-ray branching ratios and Doppler-shift information were obtained from proton-γ coincidence measurements using $BaCl_2$ targets enriched in Cl^{37}. Excitation energies were determined from singles measurements, as well as from the coincidence studies for the 10 levels previously reported in this energy range. The $J^\pi = 1^+$ level at 1942 keV, which is strongly excited in the β decay of S^{38} and which was not observed in $Cl^{37}(d,p)Cl^{38}$ studies with a magnetic spectrograph, is also weakly populated. Excitation energies (in keV) and mean lives (in psec) for the lowest 10 levels are 671.27 ± 0.16; 755.26 ± 0.11, 0.53 ± 0.18; 1308.87 ± 0.14, $1.0^{+0.9}_{-0.4}$; 1617.21 ± 0.14, $2.3^{+2.3}_{-0.9}$; 1692.4 ± 0.2, 1.9 ± 0.7; 1745.8 ± 0.3, $2.1^{+1.4}_{-0.7}$; 1785.1 ± 0.5, 0.09 ± 0.03; 1941.7 ± 0.2; 1981.11 ± 0.15, 0.43 ± 0.09; and 2743.1 ± 0.4, ≤ 0.03. The multipole strengths of the transitions linking these states with the 2^- ground state and 5^- first excited state lead in combination with the l_n transfer values from previous (d,p) work to the following spin-parity assignments: $J^\pi(755) = 3^-$; $J^\pi(1309) = 4^-$; $J^\pi(1617) = 3^-$; $J^\pi(1692) = 1^-$, 2^-, or 3^-; $J^\pi(1785) = 2^+$, 3^+, or 4^+; $J^\pi(1981) = 2^-$ or 3^-; and $J^\pi(2743) = 3^-$. The experimental results are compared with shell-model calculations and with predictions from the Pandya transformation of the known $(\pi 1d_{3/2})^{-1}(\nu 1f_{7/2})$ and $(\pi 1d_{3/2})^{-1}(\nu 2p_{3/2})$ quadruplets in K^{40}.

I. INTRODUCTION

The reaction $Cl^{37}(d, p)Cl^{38}$ has been studied by Rapaport and Buechner[1] with a multigap spectrograph using a 7.5-MeV deuteron beam and an enriched target. A total of 37 states in Cl^{38} were identified up to an excitation energy of 5.5 MeV, and numerous orbital momentum values have been assigned.

Previous studies of this reaction have also been reported in the work of Paris, Buechner, and Endt[2] and Hoogenboom, Kashy, and Buechner.[3] Electromagnetic transitions connecting the four lowest states in Cl^{38} are reported in the work of Segel *et al.*[4] These four states have $J^\pi = 2^-$, 5^-, 3^-, 4^- and arise (in first order) from the coupling of a $1f_{7/2}$ neutron to a $1d_{3/2}$ proton. The excitation energies of this quadruplet are well described[5,6] by this simple picture as is indicated also by the success of the Pandya transformation[7] on the lowest states of K^{40}. The relative $M1$ rates, however, calculated[4] within the $(\pi d_{3/2})(\nu f_{7/2})$ configurations, show discrepancies of a factor of 2 to 3 with experiment, even when effective magnetic moments are used to absorb the influence of small impurities in the wave functions. In the work of Becker and Warburton[8] it is subsequently shown that in K^{40} small admixtures of about 1% intensity of $(\pi d_{3/2})^{-1}(\nu f_{5/2})$ and $(\pi d_{5/2})^{-1}(\nu f_{7/2})$ configurations have a very large effect on the K^{40} transition rates, and their influence cannot be taken in account by the use of effective magnetic moments. It may therefore be speculated that in Cl^{38} the sensitivity of the transition rates in the $(\pi d_{3/2})(\nu f_{7/2})$ quartet to small $(\pi d_{3/2})(\nu f_{5/2})$ admixtures will show up experimentally as strong $M1$ transitions between the members of the $(\pi d_{3/2})(\nu f_{7/2})$ and $(\pi d_{3/2})(\nu f_{5/2})$ quadruplets. The latter quadruplet is expected to lie roughly about 2 MeV higher in excitation energy. However, experimental data on the γ-ray decay of the higher-lying states, which would allow an identification of this quadruplet, are not available.

Also experimentally unknown are the decay properties of the members of the $(\pi d_{3/2})(\nu p_{3/2})$ quadruplet with $J^\pi = 0^-$, 1^-, 2^-, and 3^-. Members of this multiplet cannot (in the single-configuration picture) decay by $M1$ transitions to members of the $(\pi d_{3/2})(\nu f_{7/2})$ quadruplet, but they can connect strongly among themselves. The calculations in Ref. 6 indicate that for the lowest $J^\pi = 2^-$ and 3^- states (ground state and second excited state, respectively) the admixture of the $(\pi d_{3/2})(\nu p_{3/2})$ configuration is about 2 and 15% in intensity, respectively. The considerations given above focus the attention on properties of higher excited states and were the incentive for the present work.

In the present experiment we have investigated γ-ray branchings, lifetimes, and spin assignments for Cl^{38} levels up to 2.75-MeV excitation energy. The results concerning the levels with excitation energies between 1.32 and 2.75 MeV are reported for the first time. The data obtained are compared with the predictions of the Pandya transformation of the known $(\pi 1d_{3/2})^{-1}(\nu 1f_{7/2})$ and $(\pi 1d_{3/2})^{-1}(\nu 2p_{3/2})$ quadruplets in K^{40} and with preliminary results of a large shell-model calcula-

tion by Goode.[9] In this calculation configurations of the form $(1d_{5/2}, 2s_{1/2})^{-n}(1d_{3/2})^{1+n}(\rho)$ with respect to a $_{16}S^{36}_{20}$ core were used. The symbol ρ represents a neutron in the $1f_{7/2}$, $2p_{3/2}$, or $1f_{5/2}$ shell, and the number of proton holes in the $(1d_{5/2}, 2s_{1/2})$ shell is restricted to $n=0$ or 1.

II. EXPERIMENTAL PROCEDURE AND RESULTS

A. Branching Ratios

Proton-γ coincidence spectra from the reaction $Cl^{37}(d, p\gamma)Cl^{38}$ ($Q=3.89$ MeV) were measured using a 13-cm-diam chamber, which permitted collinear detection of the reaction protons. The target consisted of $BaCl_2^{37}$, enriched to 96.1% in Cl^{37}, of about 0.5 mg/cm^2 evaporated onto a 1.1-mg/cm^2 Au foil. The deuteron beam was stopped in a 0.12-mm Mo foil. Protons resulting from the deuteron bombardment were detected by 1-mm-thick annular surface-barrier detector, placed concentric with the beam axis and subtending an angle defined by $161° \leq \theta_p \leq 170°$. A 17.1-mg/cm^2 Al absorber was placed over the front face of the detector to stop deuterons elastically scattered from the target and beam stop. Figure 1 shows the proton spectrum measured at 3.1-MeV bombarding energy. The energy resolution of about 100 keV was primarily due to the target thickness, Al absorber, and close geometry.

γ rays were detected with a coaxial 40-cm^3 Ge(Li) detector placed at $\theta_\gamma = 55°$ and located with its front face at a distance of 8.5 cm from the target. The chamber wall consisted of 0.25 mm brass at the position of the Ge(Li) detector. The front face of the Ge(Li) detector was shielded by 2 cm Lucite and the detector sides were surrounded by a lead shield of about 3.5 cm. With the indicated geometries, the particle and γ-ray detectors subtended solid angles of 2.3 and 0.9% of a sphere, respectively.

Fast-coincidence timing signals were generated by routing a signal from *each* preamplifier through a fast-timing filter amplifier and constant-fraction timing discriminator which then provided the start (on protons) and stop (on γ rays) signals for a time-to-amplitude converter. The resultant time spectrum exhibited a peak of 9 nsec full width at half maximum for γ rays of energies between 0.15 and 3.0 MeV, with a peak/random events ratio of 15/1. A time gate of 15 nsec was used throughout the measurements.

The p-γ coincidence spectrum from the detectors was recorded by a TMC 16384-channel analyzer, set to operate in a two-parameter mode of $32(p) \times 512(\gamma)$ channels. Since the result of Fig. 1 indicates that the total particle spectrum is too complex for only 32 channels, the proton spectrum was divided into three parts (corresponding to the ranges of excitation energies of 0.54–1.51, 1.47–2.15, and 2.00–2.95 MeV in Cl^{38}). Thus, three separate two-parameter spectra of $32(p) \times 512(\gamma)$ channels were accumulated with the same calibration of the γ rays. Each run lasted about 4 days. The beam current of about 350 nA was lim-

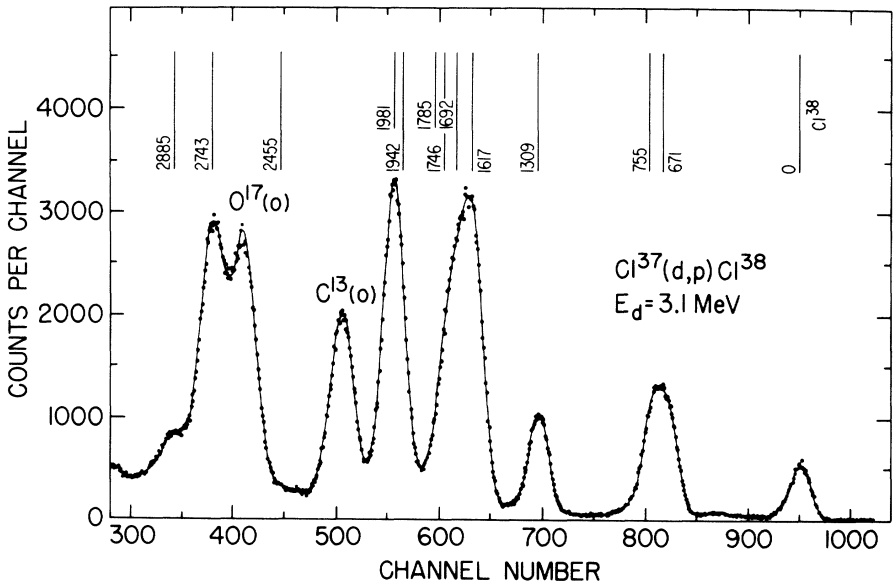

FIG. 1. Proton spectrum from the reaction $Cl^{37}(d,p)Cl^{38}$ at $E_d = 3.1$ MeV measured with a 1-mm thick annular surface-barrier detector centered at 180°. The corresponding excitation energies of states in Cl^{38} are indicated, as well as the ground-state proton groups from a carbon and oxygen contamination of the target. See also Fig. 5.

ited by the counting rate in the Ge(Li) detector.

Experimental data from these three two-parameter spectra are shown in Figs. 2 and 3, and the resulting branching ratios are given in Table I. The observation angle of $\theta_\gamma = 55°$ for the γ rays removes the influence of terms in $P_2(\cos\theta_\gamma)$. Terms in $P_4(\cos\theta_\gamma)$, if present, were neglected. The photopeak efficiency calibration of the Ge(Li) detector was determined using radioactive sources of Ba^{133}, Na^{22}, Y^{88}, and Tl^{208} placed in the chamber at the position of the target so the absorption in the thin chamber wall and in the shielding of the Ge(Li) counter is the same as in the experiment.

B. γ-Ray Energies

Singles Measurements

γ-ray singles spectra were used to determine the energies of the strongest γ-ray transitions. For these measurements, a target of about 0.5 mg/cm^2 $BaCl_2^{37}$ (on Au foil) was mounted in a glass tube, and a high-resolution Ge(Li) detector was positioned at $(90 \pm 2)°$ at a distance of about 10 cm. The beam current was kept below 40 nA to maintain optimum resolution. The mixed-source technique was used, and the spectra, with a dispersion of 0.21 keV/channel, were recorded using an 8192-channel analog-to-digital converter.

One spectrum, taken to obtain the energies of the low-energy γ rays, was recorded with a Ba^{133} source and a portion of this spectrum is shown in Fig. 4. A second spectrum was taken using sources of Mn^{54}, Cs^{137}, Ir^{192}, and Bi^{207} placed so that the intensities of the γ rays from these sources were comparable to the intensities of the reaction γ rays. A third spectrum, taken to obtain the energies of the more energetic γ rays, was accumulated together with sources of Na^{22}, Co^{60}, and Tl^{208}. In this spectrum, the well-known[10,11] 1642- and 2168-keV γ rays of Ar^{38}, from the reaction $Cl^{37}(t, d)Cl^{38}(\beta^-)Ar^{38}$, were also used for calibration.

The radioactive lines were in general chosen to form close-lying doublets with the lines of interest. The energies of the γ rays emitted by Na^{22}, Mn^{54}, Co^{60}, Cs^{137}, Ir^{192}, Bi^{207}, and Tl^{208} were taken from the compilation of Marion[12]; the Ba^{133} energies are

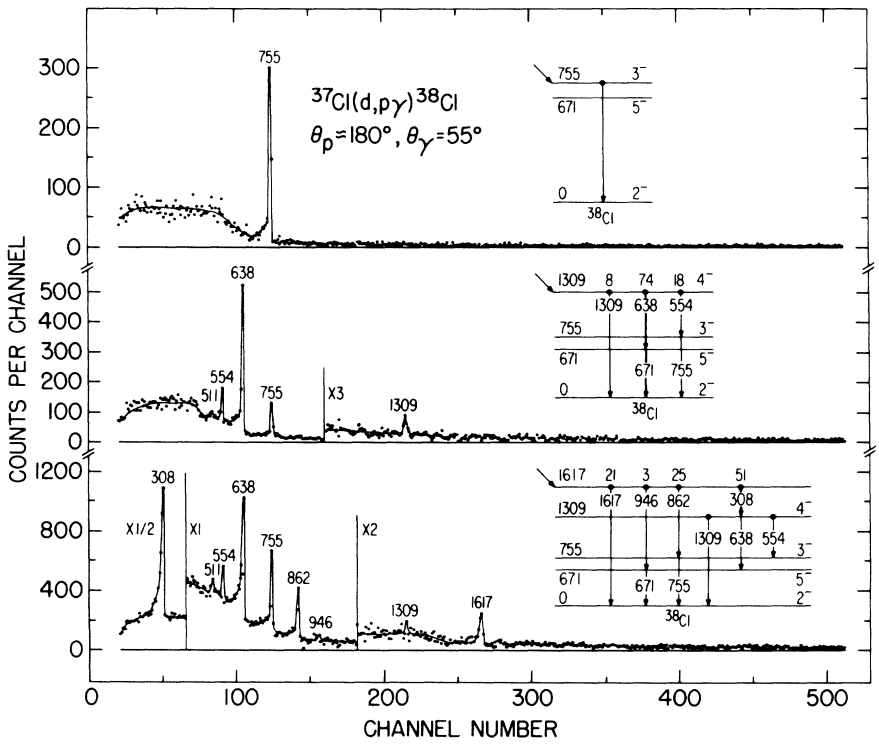

FIG. 2. Partial results of a two-parameter analysis of p-γ coincidences in the reaction $Cl^{37}(d,p\gamma)Cl^{38}$, illustrating the decay of the 755-, 1309-, and 1617-keV levels of Cl^{38}. γ rays were measured with a coaxial 40-cm^3 Ge(Li) detector at $\theta_\gamma = 55°$; the annular particle detector was centered at $\theta_p = 180°$. The various lines are identified by the γ-ray energies (in keV) and have been fitted into the Cl^{38} level scheme as shown in the insets. The branching ratios extracted from these data are given in Table I. The 671-keV state has a half-life of 0.74 sec and is therefore not observed in the coincidence data.

from Greenwood, Helmer, and Gehrke.[13] The positions of the peaks of interest were determined as follows. First, a least-squares fit of a straight line was made to the data points outside the peak region. Subsequently, a least-squares fit was made to the peak assuming a Gaussian curve superimposed on this linear background. The Gaussian fits were restricted to the channels for which the intensity was $\geq 20\%$ of the peak intensity. The next step was to fit a polynomial to the positions of the radioactive peaks of known energy. χ^2, the measure of the goodness of fit, was about unity for polynomials with degree 3, 4, or 5 and degree 4 was chosen. The results are given in column 1 of Table II. The quoted errors include the following effects: (1) uncertainties in peak position, (2) uncertainties in radioactive calibration energies, (3) uncertainty in degree of polynomial, and (4) uncertainty in the positioning of the γ detector at $\theta_\gamma = 90°$ A 2° error in position corresponds to an energy error of $\frac{2}{57}E_\gamma(v/c)f(\tau)$, where v is the velocity of the emitting Cl^{38} nucleus and $f(\tau)$ is a factor which accounts for the influence of the mean life τ. Because of cascade feeding $f(\tau)$ is smaller than or equal to $F(\tau)$, the quantity used in the lifetime measurements (see Sec. E) and given in Table IV, column 5. For the γ rays listed, this error varied between 16–300 eV. Also, due to the transverse Doppler effect, the γ-ray energy observed at 90° is systematically too low by an amount $\frac{1}{2}E_\gamma(v/c)^2$. This latter correction varied between 5 and 30 eV.

Coincidence Measurements

Some γ-ray energies were determined in p-γ coincidence measurements, as the method of the preceding paragraph is applicable only for those γ rays which were prominent and undisturbed in the singles spectrum. In the Doppler-shift measurements (see Sec. E) coincident γ-ray spectra of 2048 channels and with a dispersion of 0.79 keV/channel were recorded at $\theta_\gamma = 90°$. The energy calibration for these spectra was internal and based on the energies of six γ rays from column 1 of Table II and on the energy[14] of the 1942-keV γ ray. The results of these measurements are given in column 2 of Table II. The 671-keV γ ray was not observed in the coincidence data, in agreement with the half-life[15] of 0.74 sec for the 671-keV level. The values in column 1 and 2 of

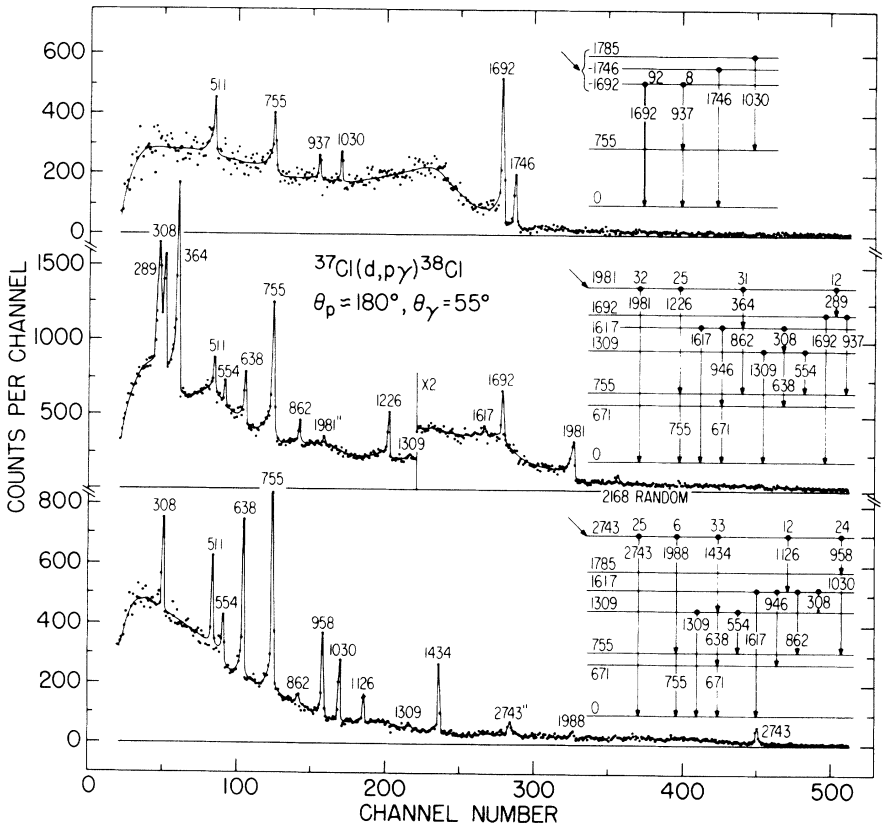

FIG. 3. Partial results of a two-parameter analysis of p-γ coincidences in the reaction $Cl^{37}(d,p\gamma)Cl^{38}$ illustrating the decay of the 1692-, 1746-, 1785-, 1981-, and 2743-keV levels of Cl^{38}. The presentation is similar to that of Fig. 2.

TABLE I. Branching-ratio information for states of Cl^{38} with $E_x < 2.8$ MeV. Branching ratios are given (in percent) for transitions from the given initial states to the indicated final states.

Final state (keV)	Initial state (keV) 671	755	1309	1617	1692	1746	1785	1942 [a]	1981	2743
0	100	100	8 ± 3	21 ± 2	92 ± 4	100	<18	100	32 ± 2	25 ± 3
671		b	74 ± 2	3 ± 2	<5	<10	<17	<0.3	<3	<5
755			18 ± 3	25 ± 2	8 ± 2	<9	100	<0.3	25 ± 2	6 ± 2
1309				51 ± 2	<5	<6	<12	<0.4	<2	33 ± 3
1617					b	b	<12	<0.4	31 ± 2	12 ± 2
1692						b	b	<0.4	12 ± 1	<2
1746							b	<0.4	<1	<2
1785								<0.4	<1	24 ± 3
1942									b	<2
1981										<2

[a] This level is very weakly populated in the present investigation and only the ground-state transition is observed. The quoted results are taken from the $S^{38}(\beta^-)Cl^{38}$ study of Ref. 14.

[b] Intensities for γ rays with energies below 150 keV cannot be extracted from these data (see Figs. 2 and 3). They are assumed to be zero.

Table II are combined in column 3, where γ-ray energies are listed for 21 transitions in Cl^{38} with errors ranging from 0.06 to 1.1 keV. The values in column 3 may be considered as independent of each other, as the relatively large errors in the energies of the coincident γ rays (column 2) are mainly due to peak-position errors and the lack of calibration points.

C. Optimum Excitation Energies

The 21 γ rays whose energies are given in column 3 of Table II correspond to transitions between 11 levels. The excitation energies of these

TABLE II. Energies and assignments (in keV) of γ rays observed in the $Cl^{37}(d, p\gamma)Cl^{38}$ reaction.

Singles $\theta_\gamma = 90°$	E_γ Coincidence $\theta_p = 180°$, $\theta_\gamma = 90°$	Adopted	Assignment in Cl^{38} $E_i \rightarrow E_f$
288.69 ± 0.06	289 ± 3	288.69 ± 0.06	1981 → 1692
308.34 ± 0.06	308 ± 3	308.34 ± 0.06	1617 → 1309
363.92 ± 0.06	364 ± 3	363.92 ± 0.06	1981 → 1617
553.58 ± 0.14	553.9 ± 0.8	553.59 ± 0.14	1309 → 755
637.60 ± 0.07	a	637.60 ± 0.07	1309 → 671
671.0 ± 1.0	...	671.0 ± 1.0	671 → 0
755.30 ± 0.12	a	755.30 ± 0.12	755 → 0
862.07 ± 0.13	a	862.07 ± 0.13	1617 → 755
...	937.0 ± 0.5	937.0 ± 0.5	1692 → 755
...	957.9 ± 0.5	957.9 ± 0.5	2743 → 1785
...	1029.6 ± 0.7	1029.6 ± 0.7	1785 → 755
...	1126.2 ± 0.9	1126.2 ± 0.9	2743 → 1617
...	1226.0 ± 0.9	1226.0 ± 0.9	1981 → 755
1434.2 ± 1.1	a	1434.2 ± 1.1	2743 → 1309
1617.2 ± 0.7	a	1617.2 ± 0.7	1617 → 0
1691.6 ± 0.4	a	1691.6 ± 0.4	1692 → 0
...	2743.5 ± 0.5 [b]	2743.5 ± 0.5	2743 → 0
1744.3 ± 1.6	1745.3 ± 0.6	1745.8 ± 0.3 [d]	1746 → 0
	c	1941.7 ± 0.2	1942 → 0
...	1980.7 ± 1.0	1980.7 ± 1.0	1981 → 0
...	1986.4 ± 0.8	1986.4 ± 0.8	2743 → 755

[a] The values of the first column are used for internal calibration.

[b] Double-escape peak.

[c] Value of 1941.7 ± 0.2 keV as given in Ref. 14 is used for internal calibration.

[d] Value of 1746.2 ± 0.4 keV as given in Ref. 14 is also taken into account.

levels are therefore overdetermined and a least-squares procedure was used to obtain their best values. First, the 21 γ-ray energies were converted into level-energy differences by adding $E_\gamma^2/2Mc^2$. Next the quantity

$$Q^2 = \sum_{i,j} [D_{ij} - (E_i - E_j)]^2/(\Delta D_{ij})^2$$

was minimized by varying the E_i. Here E_i denotes the excitation energy of level i, and D_{ij} is the experimentally measured level-energy difference between level i and level j. ΔD_{ij} represents the error in D_{ij}. The sum extends over all 21 measured D_{ij}. The best values for the E_i, and their errors, are obtained at the minimum of Q^2.

The solution of this linear least-squares problem is straightforward (see, e.g., the work of Wapstra, Nijgh, and van Lieshout[16]) and the resulting optimum excitation energies and their errors are given in column 2 of Table III. χ^2, the measure of the goodness of fit and defined as $Q^2_{\min}/(M-N)$, was 0.89. (M is the number of level-energy differences, N the number of levels.) The values for the excitation energies of the 1746- and 1942-keV levels are not affected by the least-squares procedure, as these levels decay only by ground-state transitions and are not populated by transitions from other levels (see Table I).

Column 3 of Table III gives for comparison the excitation energies obtained[1,3] with a magnetic spectrograph in the reaction $Cl^{37}(d, p)Cl^{38}$. The present results are in good agreement with this previous work, and the uncertainties are smaller by a factor of about 30.

TABLE III. Excitation energies of low-lying Cl^{38} levels.

Level No.	E_x (in keV) Present	Previous [a]
1	671.27 ± 0.16	671 ± 5
2	755.26 ± 0.11	761 ± 5
3	1308.87 ± 0.14	1309 ± 6
4	1617.21 ± 0.14	1622 ± 6
5	1692.4 ± 0.2	1695 ± 6
6	1745.8 ± 0.3	1748 ± 7
7	1785.1 ± 0.5	1790 ± 8
8	1941.7 ± 0.2 [b]	...
9	1981.11 ± 0.15	1986 ± 7
10	... [c]	2461 ± 12
11	2743.1 ± 0.4	2752 ± 12

[a] $Cl^{37}(d, p)Cl^{38}$ at $E_d = 7.5$ MeV with magnetic spectrograph. The energies for levels Nos. 1 through 9 are taken from Ref. 3 and for levels Nos. 10 and 11 from Ref. 1.

[b] Value taken from Ref. 14.

[c] Not observed in this experiment.

D. Population of the 1^+ 1942-keV Level

The β^- decay of S^{38} proceeds mainly[14] (83%) via an allowed transition to the Cl^{38} level at 1942 keV, and until now this level has not been observed in other reactions. As the ground state of S^{38} is in the $[(d_{3/2})^4{}_{02}(f_{7/2})^2{}_{01}]_{J=0\ T=3}$ configuration with an amplitude[17] of 87%, the allowed β decay indicates then for the 1942-keV level a $(d_{3/2})^4(f_{7/2})^2$ configuration, which would explain why this level until now has escaped detection in the reaction[1-3] $Cl^{37}(d, p)Cl^{38}$, since the Cl^{37} ground state is dominated by the $(d_{3/2})^5$ configuration[6] with an amplitude of about 95%.

Figure 5 shows some data from one of the two-parameter p-γ coincidence runs described in Sec. A. The spectrum at the top represents the proton spectrum coincident with all γ rays and corresponds to excitation energies between 1.47 and 2.15 MeV in Cl^{38}. The lower spectra are proton spectra coincident with γ rays specific to the decay of a particular level (see Figs. 2, 3, and Table I), and show that the two broad peaks in the top spectrum actually consist of six peaks, thus demonstrating the powerful features of the two-parameter mode. As the evidence for a proton group corresponding to the 1942-keV level is rather weak, the following additional experiment was performed. A voltage gate was set for proton pulses corresponding to 1.85–2.15-MeV excitation in Cl^{38} and the coincident γ rays were detected at 90° and

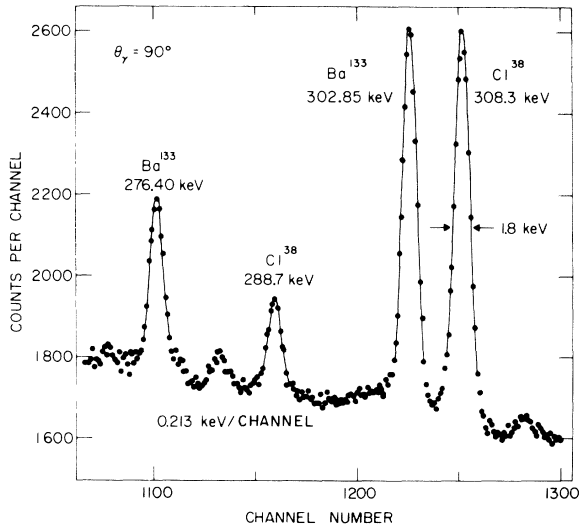

FIG. 4. Portion of a 20-cm^3 Ge(Li) spectrum obtained from 3.1-MeV deuteron bombardment of a 0.5 mg/cm^2 $BaCl_2^{37}$ target on gold. The detector was at 90° with respect to the beam and 10 cm from the target. The energies of the Cl^{38} peaks are based on those given for the Ba^{133} peaks. Detailed information is given in Table II and in the text.

accumulated in 2048 channels with a dispersion of 0.79 keV/channel. A portion of the coincidence data from the second 1024 channels is presented in Fig. 6 and shows clearly the 1942-keV γ ray which characterizes[14] the decay of the 1942-keV state, thus demonstrating that the $J^\pi = 1^+$ level at 1942 keV is weakly populated in the (d, p) reaction. The remote possibility of a 1981 → 1942-keV γ-ray transition can be ruled out on the basis of spin assignments and the lifetime of the 1981-keV level (see Sec. E).

The population of the 1942-keV level at this low bombarding energy of $E_d = 3.1$ MeV is probably due mainly to compound effects. However, population of this level in a direct process would indicate the presence of $(f_{7/2})^2$ configurations in the Cl^{37} ground state, as shown schematically in Fig. 7. This question could be settled by performing a (d, p) stripping experiment to this level at say, e.g., $E_d = 12$ MeV. The spectroscopic factor for this $l = 2$ transfer would then determine the amplitude of this two-particle–five-hole admixture in the ground state of Cl^{37}.

E. Lifetime Measurements

The experimental setup was, apart from minor changes, identical to that used in the measurement of the branching ratios (see Sec. A). Two $BaCl_2^{37}$ targets, 280 ± 30 and 520 ± 50 $\mu g/cm^2$ thick, on a 42-mg/cm^2 Ta backing were used. Their uniformity was better than 10%. The thickness of the thinner target was measured at the strong Cl^{37}-$(p, \gamma)Ar^{38}$ analog resonance[10] at $E_p = 1732$ keV, while that of the thicker target was determined relative to this by comparison of the proton yields in the (d, p) reaction.

For these measurements the annular particle detector was set to subtend a slightly larger solid angle defined by $161° \leq \theta_p \leq 174°$. Under these conditions the Cl^{38} ions were restricted to move in a forward cone with a half angle of 9°, with a velocity of about $v/c = 0.55\%$ (see Table IV). The beam current was kept at about 50 nA to maintain optimum resolution for the Ge(Li) detector. The TMC analyzer was *now* used in a spectrum-sort mode in order to have more channels available for the γ-ray spectrum analysis. In this mode spectra of

TABLE IV. Mean lives of Cl^{38} states.

E_x (keV)	E_γ (keV)	Measured shift $0-90°$ (keV)	$\frac{v}{c}$ [a] (%)	F [b] (%)	τ Present (psec)	τ Previous [c] (psec)
755	755	1.5 ± 0.3	0.58	35 ± 7	0.53 ± 0.18	$0.35^{+0.20}_{-0.15}$
1309	638	0.8 ± 0.3	0.57	22 ± 9	$1.0^{+0.9}_{-0.4}$	1.0 ± 0.3
1617	862	0.4 ± 0.3	0.56	8 ± 7	$2.3^{+2.3}_{-0.9}$	2.2 ± 0.2 [d]
	1617	1.0 ± 0.5	0.56	11 ± 6		
1692	1692	1.1 ± 0.3	0.56	12 ± 3	1.9 ± 0.7	
1746	1746	1.1 ± 0.4	0.56	11 ± 4	$2.1^{+1.4}_{-0.7}$	
1785	1030	4.3 ± 0.8	0.56	75 ± 14	0.09 ± 0.03	
	1030 [e]	4.3 ± 0.3	0.53	79 ± 6		
1981	1226	2.5 ± 0.2	0.55	37 ± 3	0.43 ± 0.09	0.56 ± 0.08 [d]
	1981	4.4 ± 0.3	0.55	41 ± 3		
2743	958	5.2 ± 0.3	0.53	102 ± 6	≤ 0.03	
	1126	5.8 ± 0.4	0.53	98 ± 7		
	1434	7.5 ± 0.3	0.53	100 ± 4		

[a] Calculated from the kinematics. Small corrections due to carbon build up and target thickness are taken into account. The over-all uncertainty is less than 0.01.

[b] Ratio of the observed shift to the unattenuated shift for a target consisting of 0.52 mg/cm^2 $Ba^{37}Cl_2$ on 42 mg/cm^2 Ta.

[c] Reference 4.

[d] Result of a Doppler-shift measurement with the reaction $H^2(Cl^{37}, p)Cl^{38}$, see Ref. 28.

[e] In this case the 1785-keV level was populated via the short-lived 2743-keV level.

2048 channels from one detector can be recorded in coincidence with up to eight digital voltage gates set on the other.

In the proton spectrum shown in Fig. 1, six digital gates were set corresponding to excitation energies in Cl^{38} of 0.62–0.90, 1.20–1.42, 1.52–1.81, 1.88–2.06, 2.13–2.31, and 2.64–2.85 MeV. Coincidence data, each consisting of six 2048-channel spectra with a dispersion of 0.79 keV/channel, were accumulated using the 520-$\mu g/cm^2$ target, with the Ge(Li) detector successively at $\theta_\gamma = 90$, 0, and 90° again. Two such spectra were recorded at $\theta_\gamma = 0$ and 90° with the 280-$\mu g/cm^2$ target. The measurement at $\theta_\gamma = 0°$ with the 280-$\mu g/cm^2$ target served primarily as a check on the measurements as well as on the analysis. The accumulation of the Doppler-shift data took about 11 days and was greatly facilitated by an automatically controlled accelerator, which ran unattended during most of this period.

The three spectra obtained at $\theta_\gamma = 90°$ were summed together after small corrections for gain and base-line shifts were made by computer. Results are shown in Figs. 8 and 9. Due to the long duration of the measurements and small instabilities in the electronics, the 90° data have (in the analysis) to be adjusted with respect to the 0° data in order to determine the 0–90° Doppler shift for the several γ rays. This, in general unknown, adjustment is a disadvantage of the method as compared to coincident Doppler-shift techniques in which use is made of one Ge(Li) detector, two particle detectors, and one[18, 19] or two[20–22] targets. In this particular case, however, the adjustment of the 90° data is facilitated by the appearance of a number of intense "stopped peaks" in the 0° data due to the relatively long lifetimes of some of the levels involved (see Figs. 8–10).

The next step in the analysis was the determination of the centroids of the γ-ray distributions at 0 and 90° and the calculation of $F(\tau)$ defined as $F(\tau) = (\Delta E_\gamma)_{exp}/(\Delta E_\gamma)_{\tau=0}$. Here $(\Delta E_\gamma)_{exp}$ denotes the experimental measured shift and $(\Delta E_\gamma)_{\tau=0}$ the shift which would have been observed for an infinitely short mean life. The latter was calculated from the kinematics, and small corrections due to carbon buildup on the target, target thickness, and the solid angle of the Ge(Li) detector are taken into account. Results are given in Table IV.

For the 1617-, 1981-, and 2743-keV levels, it is shown in column 5 of Table IV that the same $F(\tau)$ is obtained for energetically quite different γ rays deexciting the same level; thus providing a check on the adjustment procedure of the 90° data described above. Another check on this point is obtained from the analysis of the 0° line shape of the 1226-, 1692-, and 1981-keV γ rays, shown

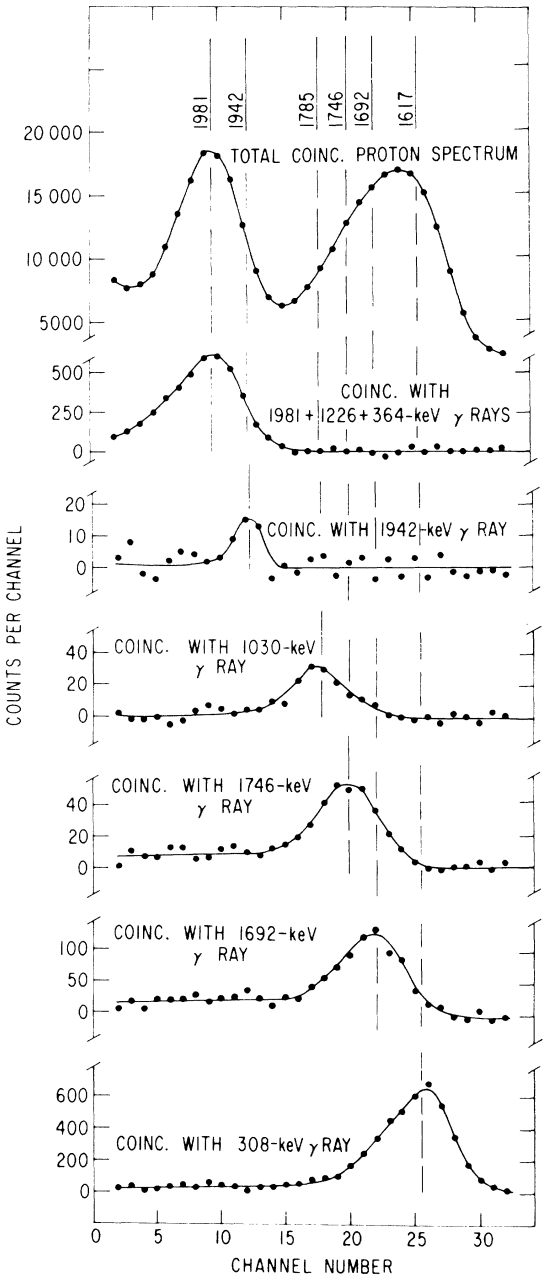

FIG. 5. Partial results of a two-parameter analysis of p-γ coincidences in the reaction $Cl^{37}(d,p\gamma)Cl^{38}$ measured at $E_d = 3.1$ MeV. The plot at the top shows the proton spectrum measured in coincidence with all γ-ray pulses of energy $E_\gamma > 150$ keV. The lower plots show the proton spectra measured in coincidence with specific γ rays which characterize the decay of various states of Cl^{38}. The proton peaks are identified by the excitation energies (in keV) of the Cl^{38} levels to which they correspond. Protons were observed with an annular surface-barrier detector centered at 180°, while γ rays were detected by a 40-cm^3 Ge(Li) detector placed at 55°. Supporting evidence for the population of the 1942-keV state is shown in Fig. 6.

in Fig. 10 and described below. The $F(\tau)$ values determined solely from the line shapes measured at 0° are in good agreement with the $F(\tau)$ values obtained from the 0–90° shift.

Theoretical curves of $F(\tau)$ were calculated from the ion energy-loss relationships of Lindhard, Scharff, and Schiøtt (LSS)[23] utilizing the Blaugrund treatment.[24] The exponent p in the electronic stopping power was kept fixed at 0.50. The parameter ξ_e, which is independent[25] of the stopping medium and has the value of $Z_1^{1/6} = 1.604$ in the LSS theory, was taken as 1.25 $Z_1^{1/6}$ for both $BaCl_2$ and Ta stopping media. As indicated by the work of Ormrod, MacDonald, and Duckworth[25] and Fastrup *et al.*[26,27] this value is appropriate for Cl ions over the velocity range of $v/c = (0–0.55)\%$. It can be seen from Fig. 11 that the computed $F(\tau)$ curves for Cl^{38} ions slowing down in pure $BaCl_2^{37}$ and in pure Ta are very different, and it is, therefore, obviously important to take the target thickness correctly into account. This was done using a computer program in which the 520-$\mu g/cm^2$ $BaCl_2$ target was divided into 20 layers, and the corresponding $F(\tau)$ for slowing down in $BaCl_2^{37}$ and Ta was calculated for each layer. The resultant (average) curve of $F(\tau)$ vs τ is also shown in Fig. 11. Results are given in Table IV, which includes also, for comparison, some recent other measurements of Cl^{38} lifetimes.[4,28]

For several of the higher-energy transitions, the Doppler shift at $\theta_\gamma = 0°$ was sufficiently large (relative to the detector resolution) that distinct line shapes were observed, as illustrated in Fig. 10. For these cases a phenomenological representation of the ion slowing-down process was assumed, as discussed previously,[29,30] in order to calculate the theoretical line shapes for various values of τ. The form used is $dE/dx = K_n(v/v_0)^{-1}$

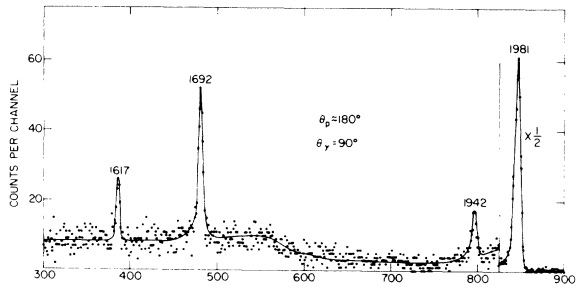

FIG. 6. Portion of the γ-ray spectrum measured in coincidence with proton groups leading to states in Cl^{38} with excitation energies between 1.85–2.15 MeV. The spectrum was recorded at $\theta_\gamma = 90°$ with a dispersion of 0.79 keV/channel and shows clearly the 1942-keV γ ray which characterizes the decay of the 1942-keV level of Cl^{38}.

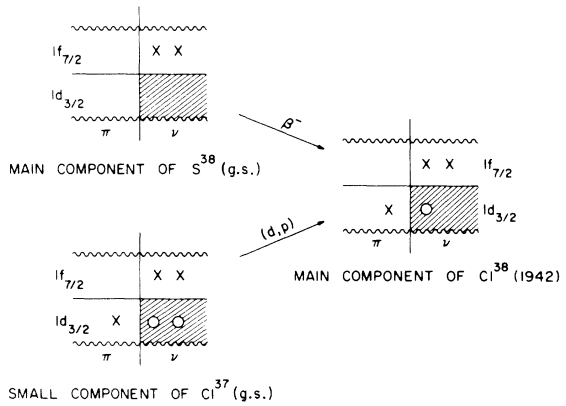

FIG. 7. First-order picture of the β^- decay from the S^{38} ground state to the Cl^{38} level at 1942 keV and of the $Cl^{37}(d,p)$ reaction leading to the same state. Population of the 1942-keV level in a direct process depends on the amplitude of the $(1d_{3/2})^3(1f_{7/2})^2$ configuration in the Cl^{37} ground state, which is dominated by the $(1d_{3/2})^5$ configuration. See text.

$+K_e(v/v_0) - K_3(v/v_0)^3$. Here the first two terms parametrize the nuclear and electronic stopping cross sections, respectively, and $v_0 = c/137$. The term in $(v/v_0)^3$ is important only for large velocities and was set equal to zero. With this representation one obtains an analytic expression for the line shape in terms of the parameters τ, K_e, K_n, and the 0–90° Doppler shift ΔE_K defined by the reaction kinematics.

The solid curves of Fig. 10 show the theoretical line shapes (after folding in an appropriate resolution function) calculated for the indicated mean lives. Here $\Delta E_K = E_K - E_0$, where E_K is the maximum Doppler-shift energy, and E_0 is the at-rest energy of the transition. The target was represented as n layers ($n = 9$ was sufficient) of $BaCl_2^{37}$, 520 $\mu g/cm^2$ thick, on a Ta backing. For each medium K_e was taken to give an electronic stopping power 1.25 × the Lindhard-Scharff-Schiøtt estimate, as discussed above, while K_n was set equal to Bohr's estimate[30] of the nuclear stopping power at $v/v_0 = 1$. Justification for this procedure has been given previously.[30] As illustrated, quite acceptable fits are obtained for values of τ consistent with the values obtained in the preceding analysis. The dashed curve shown in Fig. 10 for the 1981 → 0 transition illustrates the decomposition of the computed line shape into the "stopped component" at E_0 and the "fast component" which extends towards E_K.

The mean lives given in Table IV lead in combination with the branching ratios of Table I to the partial γ-decay widths given in Table V (column 2). The corresponding transition strengths for $E1$, $M1$, $E2$, $M2$, and $E3$ radiation are given

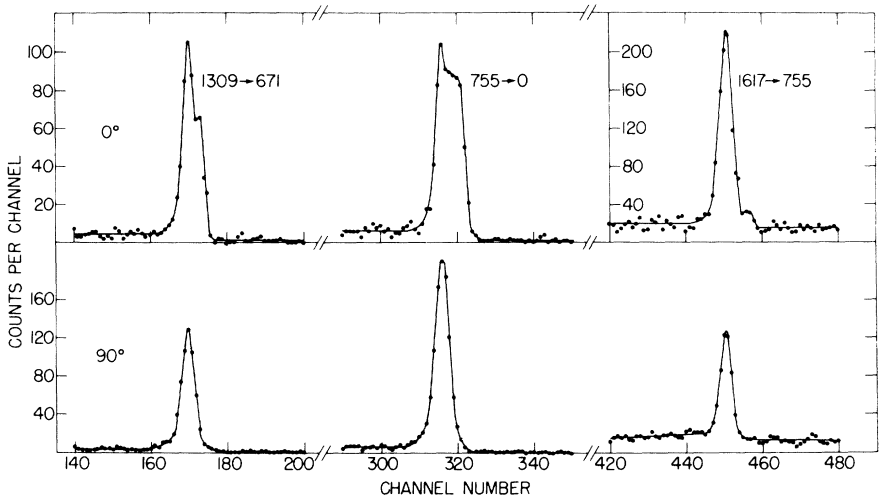

FIG. 8. Doppler-shift data from the reaction $Cl^{37}(d,p\gamma)Cl^{38}$ for primary γ rays measured in coincidence with the proton groups leading to the 755-, 1309-, and 1617-keV states of Cl^{38}. The proton detector, centered at 180°, restricted the Cl^{38} ions to move in a forward cone with a half angle of 9°, with a velocity of about $v/c = 0.55\%$. The 40-cm^3 Ge(Li) detector was positioned at 0° (upper spectra) or at 90° (lower spectra), and the dispersion is 0.79 keV/channel. The 0–90° shifts extracted from these data are given in Table IV. A target of 0.52 mg/cm^2 $BaCl_2^{37}$ on 42 mg/cm^2 Ta was used.

in Weisskopf units (W.u.) in columns 3–7 and are calculated under the assumption that the transitions are pure. The rejection of transition strengths with $|M(E2)|^2 \geq 190$ W.u. or $|M(M2)|^2 \geq 70$ W.u. or $|M(E3)|^2 \geq 60\,000$ W.u. (which on the basis of observed systematics[31] is quite conservative) leads to the multipole restrictions given in column 8 of Table V. The lowest-order multipole consistent with the spin and parity assignments discussed in the next section is denoted in Table V by underlining the corresponding transition strengths.

In this respect we note that the measured lifetimes determine that the strong $M1$ transitions, 1617 → 1309, 1981 → 1617, and 1981 → 1692 keV, must have mixing ratios close to zero, as $E2$ admixtures of 20 W.u. would correspond to mixing ratios of $|x| = 0.05$, 0.04, and 0.04, respectively.

III. DISCUSSION

A. Spin and Parity Assignments

The multipole restrictions in column 8 of Table V lead, in combination with the l_n transfer values from previous (d, p) work[1] and the known J^π values for the ground and first excited state, to spin and parity assignments for several levels, as discussed below. The $J^\pi = 2^-$ and 5^- assignments to the ground and first excited state in Cl^{38}, respectively, are discussed in Ref. 15.

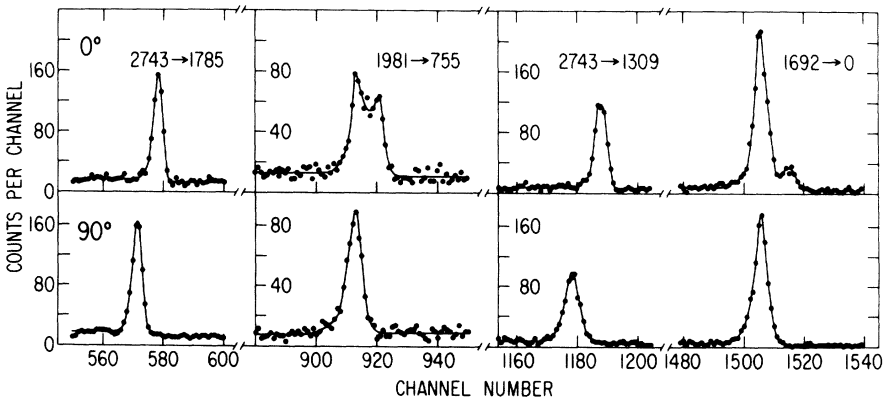

FIG. 9. Doppler-shift measurement in the reaction $Cl^{37}(d,p\gamma)Cl^{38}$ for primary γ rays measured in coincidence with proton groups leading the 1692-, 1981-, and 2743-keV levels in Cl^{38}. See caption of Fig. 8.

The 1309-keV Level

The strength of the 1309 → 671-keV transition limits the spin of the 1309-keV level to $J_{1309}=4$, 5, or 6. The 1309 → 0-keV transition restricts the spin to $J^{\pi}_{1309} \leq 4^-$. Thus we conclude for this level that $J^{\pi}_{1309}=4^-$. Note that the observed ground-state branch cannot arise from summing of the 638- and 671-keV γ rays, since the 671-keV isomeric state has a half-life of $T_{1/2}=0.74$ sec.[32] The observed $l_n=3$ value also supports the conclusion $J^{\pi}=4^-$. This assignment has been previously suggested in Refs. 1–3 and is in agreement with the observation of its $J^{\pi}=4^-$ analog[10] in Ar^{38}.

The 755-keV Level

The strength of the 755 → 0-keV transition limits the spin of the 755-keV level to $J_{755}=1$, 2, or 3. The 1309 → 755-keV transition restricts the spin to $J_{755}=3$, 4, or 5 and thus we conclude $J_{755}=3$. The $l_n=1+3$ value determines the parity as negative. A $J^{\pi}=3^-$ assignment has been previously suggested in Refs. 1–3 and is in agreement with the observation of its $J^{\pi}=3^-$ analog[33,10] in Ar^{38}.

The 1617-keV Level

The strength of the 1617 → 1309-keV transition limits the spin of the 1617-keV level to $J_{1617}=3$, 4, or 5. The 1617 → 0-keV transition restricts the spin to $J \leq 4$, thus we have jointly $J_{1617}=3$ or 4. The $l_n=1$ value determines the parity as negative and restricts the spin to $J^{\pi}_{1617} \leq 3^-$. The only assignment consistent with these restrictions is $J^{\pi}_{1617}=3^-$.

The 1692-keV Level

The strength of the 1692 → 0-keV transition limits the spin of the 1692-keV level to $J^{\pi}_{1692}=0^-$, 1, 2, 3, or 4^-. The 1692 → 755-keV transition restricts the spin to $J^{\pi} \geq 1^-$. The $l_n=1$ value determines the parity as negative and restricts the spin to $J^{\pi}_{1692}=0^-$, 1^-, 2^-, or 3^-. The combined conclusion is therefore $J^{\pi}_{1692}=1^-$, 2^-, or 3^-. A speculative assignment of 1^- is given in Ref. 3 on the basis of the observed stripping strength. This assignment is supported by the Pandya transformation[7] of the known[34] $(\pi 1d_{3/2})^{-1}(\nu 2p_{3/2})$ multiplet in K^{40} (see Sec. III C).

TABLE V. Radiative widths and electromagnetic transition strengths in Cl^{38}.

Transition (MeV)	Partial Γ_γ [a] (eV)	Transition strengths [b] (Weisskopf units) $E1$	$M1$	$E2$	$M2$	$E3$	Restrictions on J and π
0.755 → 0	1.2×10^{-3}	3.6×10^{-3}	0.13	7.8×10^{2}	2.8×10^{4}		$\Delta J \leq 1$
1.309 → 0	5.3×10^{-5}	0.3×10^{-4}	0.0011	2.2	81	2.4×10^{5}	$\Delta J \leq 2$, no $M2$
1.309 → 0.671	4.9×10^{-4}	2.5×10^{-3}	0.091	7.4×10^{2}	2.8×10^{4}		$\Delta J \leq 1$
1.309 → 0.755	1.2×10^{-4}	0.9×10^{-3}	0.034	3.7×10^{2}	1.4×10^{4}		$\Delta J \leq 1$
1.617 → 0	6.0×10^{-5}	0.2×10^{-4}	0.0007	0.9	32	6.2×10^{4}	$\Delta J \leq 2$
1.617 → 0.671	0.9×10^{-5}	1.4×10^{-5}	0.0005	1.9	70	4.0×10^{5}	$\Delta J \leq 2$, no $M2$
1.617 → 0.755	7.2×10^{-5}	1.5×10^{-4}	0.0054	24	900	6.2×10^{6}	$\Delta J \leq 2$, no $M2$
1.617 → 1.309	1.5×10^{-4}	6.7×10^{-3}	0.24	8.6×10^{3}	3.2×10^{5}		$\Delta J \leq 1$
1.692 → 0	3.2×10^{-4}	0.9×10^{-4}	0.0031	3.7	136	2.4×10^{5}	$\Delta J \leq 2$, no $M2$
1.692 → 0.755	2.8×10^{-5}	0.4×10^{-4}	0.0016	6.2	228	1.3×10^{6}	$\Delta J \leq 2$, no $M2$
1.746 → 0	3.1×10^{-4}	0.8×10^{-4}	0.0028	3.1	113	1.9×10^{5}	$\Delta J \leq 2$, no $M2$
1.785 → 0.755	7.3×10^{-3}	8.7×10^{-3}	0.32	1.0×10^{3}	3.7×10^{4}		$\Delta J \leq 1$
1.981 → 0	4.9×10^{-4}	0.8×10^{-4}	0.0030	2.6	95	1.2×10^{5}	$\Delta J \leq 2$, no $M2$
1.981 → 0.755	3.8×10^{-4}	2.7×10^{-4}	0.0098	22	810	2.8×10^{6}	$\Delta J \leq 2$, no $M2$
1.981 → 1.617	4.7×10^{-4}	1.3×10^{-2}	0.46	1.2×10^{4}	4.3×10^{5}		$\Delta J \leq 1$
1.981 → 1.692	1.8×10^{-4}	9.7×10^{-3}	0.36	1.4×10^{4}	5.3×10^{5}		$\Delta J \leq 1$
2.743 → 0	$\geq5.5\times10^{-3}$	$\geq3.5\times10^{-4}$	$\geq$0.013	≥5.7	≥212	$\geq1.4\times10^{5}$	$\Delta J \leq 2$, no $M2$
2.743 → 0.755	$\geq1.3\times10^{-3}$	$\geq2.2\times10^{-4}$	$\geq$0.0079	≥6.7	≥247	$\geq3.2\times10^{5}$	$\Delta J \leq 2$, no $M2$
2.743 → 1.309	$\geq7.2\times10^{-3}$	$\geq3.2\times10^{-3}$	$\geq$0.12	$\geq1.9\times10^{2}$	$\geq0.7\times10^{4}$		$\Delta J \leq 1$
2.743 → 1.617	$\geq2.6\times10^{-3}$	$\geq2.4\times10^{-3}$	$\geq$0.087	$\geq2.3\times10^{2}$	$\geq0.8\times10^{4}$		$\Delta J \leq 1$
2.743 → 1.785	$\geq5.3\times10^{-3}$	$\geq7.8\times10^{-3}$	≥0.29	$\geq1.0\times10^{3}$	$\geq3.9\times10^{4}$		$\Delta J \leq 1$

[a] As computed for the branching ratios of Table I and the mean lives summarized in Table IV.

[b] The lowest possible multipole which is in agreement with spin and parity assignments based on this and previous experiments is underlined.

The 1785-keV Level

The strength of the 1785 → 755-keV transition limits the spin of the 1785-keV level to $J_{1785}=2$, 3, or 4, while the $l_n=2$ value determines the parity as positive.

The 1981-keV Level

The strength of the 1981 → 1617-keV transition limits the spin of the 1981-keV level to $J_{1981}=2$, 3, or 4. The $l_n=1$ value determines the parity as negative and restricts the spin to $J^{\pi}_{1981}=0^-$, 1^-, 2^-, or 3^-. Thus we conclude $J^{\pi}_{1981}=2^-$ or 3^-. The Pandya transformation of the $(\pi 1d_{3/2})^{-1}(\nu 2p_{3/2})$ multiplet in K^{40} suggests a 2^- assignment (see Sec. III C).

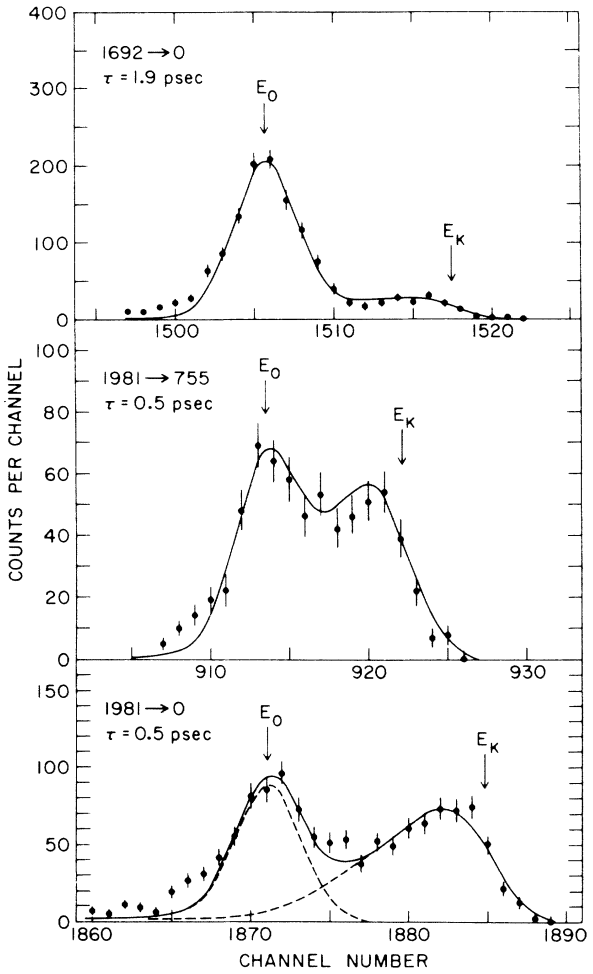

FIG. 10. Doppler-shift line shapes observed in the reaction $Cl^{37}(d,p\gamma)Cl^{38}$ for γ rays measured in coincidence with proton groups leading to the 1692- and 1981-keV states of Cl^{38}. These spectra were taken with the 40-cm^3 Ge(Li) detector positioned at 0° at 8.5-cm distance and with a dispersion of 0.79 keV/channel. The proton detector, centered at 180°, restricted the Cl^{38} ions to move in a forward cone with a half angle of 9°, with a velocity of about $v/c=0.55\%$. A linear background has been subtracted from the data. The solid curves are theoretical fits to the line shapes for the indicated value of the mean life. A phenomenological representation of the ion slowing-down process, described in the text, was used in these calculations. The full kinematic shift is given by E_k-E_0.

The 2743-keV Level

The strength of the 2743 → 1309-keV transition limits the spin of the 2743-keV level to $J_{2743}=3$, 4, or 5, while that of the 2743 → 0-keV transition restricts the spin to $J^{\pi}_{2743}=0^-$, 1, 2, 3, or 4^-. The combined restriction is therefore $J^{\pi}_{2743}=3$ or 4^-. The $l_n=1$ value determines the parity as negative and restricts the spin to $J^{\pi}_{2743}\leq 3^-$. Thus we conclude $J^{\pi}_{2743}=3^-$. The 2743-keV level is strongly populated in the reaction $Ar^{40}(p, He^3)Cl^{38}$ (see Fig. 8 of the work of Hardy, Brunnader, and Cerny[35]), as well as in the reaction $Ar^{40}(d, \alpha)Cl^{38}$.[36] Since the parity of this level is negative, it must be formed by pickup of two nucleons from different orbits in Ar^{40}. The ratio of experimental cross sections observed in the (p, He^3) and (p, t) reactions for the 2743-keV level and its analog in Ar^{38} at 13.332 MeV is consistent with this inference. The (p, t) selection rule indicates[36] for the Ar^{38} analog state (and therefore also for the 2743-keV Cl^{38} level) a $J^{\pi}=1^-$ or 3^- assignment, in agreement with the conclusion $J^{\pi}=3^-$ given above. The

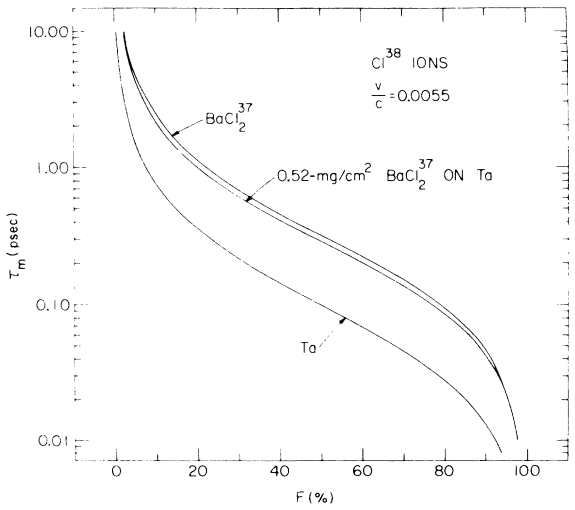

FIG. 11. The Doppler shift (expressed as a fraction F of the full shift) given as a function of the mean life τ_m. The curves were computed from the theory mentioned in Sec. E, for Cl^{38} ions slowing down in pure $BaCl_2^{37}$, pure Ta, and 0.52 mg/cm^2 $BaCl_2^{37}$ on Ta. For the latter computation the target was divided into 20 layers and a constant cross section was assumed throughout the target.

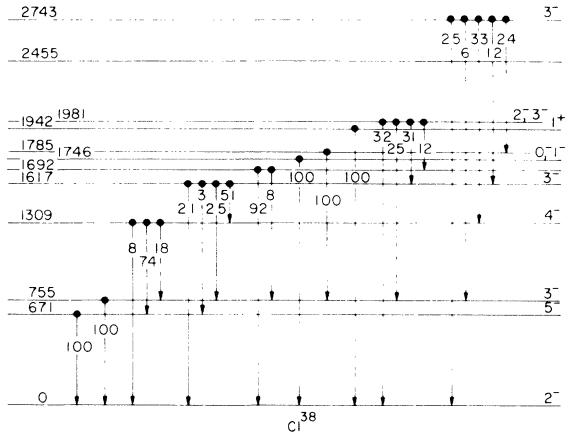

FIG. 12. Summary of excitation energies, branching ratios, and spin assignments of Cl^{38} levels below an excitation energy of 2.75 MeV. The 1692-keV level has $J^\pi = 1^-$, 2^-, or 3^-, while the 1785-keV level is restricted to $J^\pi = 2^+$, 3^+, or 4^+. Detailed information is found in Tables I and III and in Sec. III A.

spin assignments and decay modes are summarized in Fig. 12.

B. Mixing Between the $(\pi 1d_{3/2})(\nu 1f_{7/2})$ and $(\pi 1d_{3/2})(\nu 2p_{3/2})$ Quadruplets

For quadruplets of pure $(\pi 1d_{3/2})(\nu 1f_{7/2})$ and $(\pi 1d_{3/2})(\nu 2p_{3/2})$ configurations one expects strong $M1$ transitions between members of the same quadruplet[10,37] and no $M1$ strength between members of different quadruplets. This simple picture will be distorted, however, by: (1) mixing of the $(d_{3/2}f_{7/2})$ and $(d_{3/2}p_{3/2})$ configurations for the $J^\pi = 2^-$ and 3^- states, and (2) admixtures from other configurations. How far the simple picture is retained can be judged from Table VI, where the $M1$ decay strengths of $(\pi 1d_{3/2})(\nu 2p_{3/2})$ states are given. The two "interquadruplet" $M1$ transitions are almost 2 orders of magnitude stronger than the transitions linking members of different quadruplets, with the exception of the 1617-keV ($J^\pi = 3^-$) → 1309-keV ($J^\pi = 4^-$) transition. This strong transition is most likely due to a large $(d_{3/2}f_{7/2})$ admixture in the $J^\pi = 3^-$, $(d_{3/2}p_{3/2})$-quadruplet state as indicated already by the wave function calculated in Ref. 6, which gives a $(d_{3/2}f_{7/2})$ admixture of about 40% in amplitude. This is directly related to the $(d_{3/2}p_{3/2})$ admixture in the $J^\pi = 3^-$, $(d_{3/2}f_{7/2})$-quadruplet state at 755 keV, which admixture experimentally shows up as an $l_n = 1 + 3$ transfer value in the (d, p) reaction.[1]

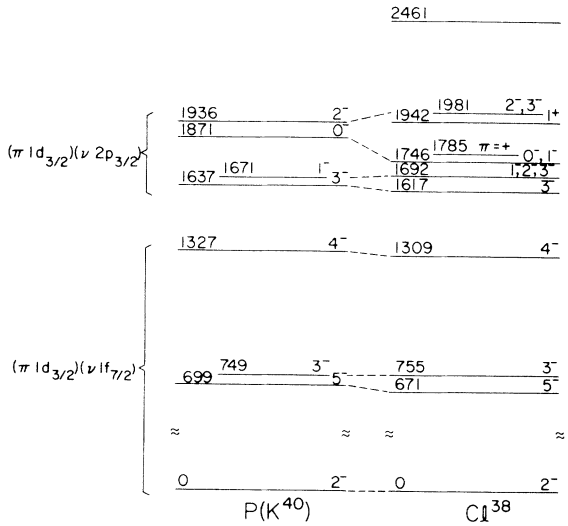

FIG. 13. Comparison of the observed Cl^{38} level scheme with that derived from K^{40} by use of the Pandya transformation. Details are given in Sec. III C.

C. Pandya Transformation of the $(\pi 1d_{3/2})(\nu 1f_{7/2})$ and $(\pi 1d_{3/2})(\nu 2p_{3/2})$ Quadruplets of K^{40}

In 1956 it was shown by Pandya and independently by Goldstein and Talmi[7] that excitation energies in Cl^{38} and K^{40} are related linearly if Cl^{38} and K^{40} are described in a particle-particle and particle-hole picture, respectively. The Pandya transformation is given by the relationship

$$E_{J'} = -\sum_J (2J+1) E_J W(j_1 j_2 j_2 j_1, J'J), \tag{1}$$

with j_1 and j_2 denoting the proton and neutron orbit, respectively. Equation (1) leads for the $(\pi 1d_{3/2})(\nu 1f_{7/2})$ quadruplets ($j_1 = \frac{3}{2}$, $j_2 = \frac{7}{2}$) to the relations given explicitly by Goldstein and Talmi.[7]

The $(\pi 1d_{3/2})(\nu 2p_{3/2})$ quadruplets ($j_1 = \frac{3}{2}, j_2 = \frac{3}{2}$) in both nuclei are related under the Pandya transformation by the following equations:

$$10(E_2^{Cl} - E_3^{Cl}) = 5(E_0^K - E_2^K) + 3(E_1^K - E_2^K) - 3(E_3^K - E_2^K), \tag{2}$$

TABLE VI. $M1$ transition strengths for members of $(\pi 1d_{3/2})(\nu 2p_{3/2})$ quadruplet in Cl^{38}.

Type [a]	$E_i \rightarrow E_f$ (keV)	$M1$ Strength (W.u.)
W	1617 → 0	0.0007
	1617 → 755	0.0054
	1617 → 1309	0.24
	1692 → 0	0.0031
	1981 → 0	0.0030
	1981 → 755	0.0098
S	1981 → 1671	0.46
	1981 → 1692	0.36

[a] W denotes $M1$ transitions linking $(\pi 1d_{3/2})(\nu 2p_{3/2})$ and $(\pi 1d_{3/2})(\nu 1f_{7/2})$ members, while S denotes $M1$ transitions between $(\pi 1d_{3/2})(\nu 2p_{3/2})$ members only.

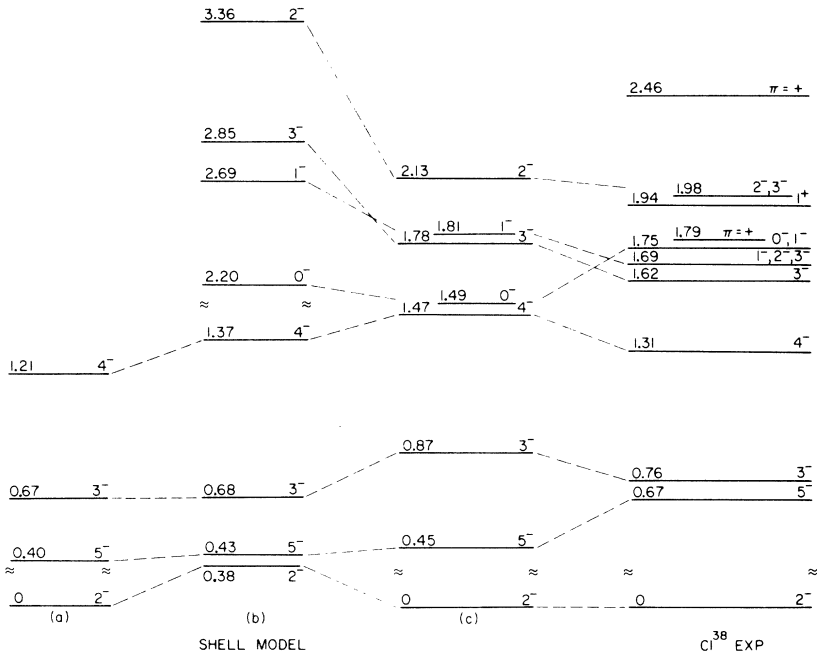

FIG. 14. Comparison of the observed Cl^{38} level scheme with shell-model calculations of increasing configuration space. The suggestion of spins 1^-, 0^-, and 2^- for levels at 1.69, 1.75, and 1.98 MeV, respectively, is in agreement with the results of the Pandya transformation of the $(\pi 1d_{3/2})(\nu 2p_{3/2})$ quadruplet in K^{40}. Details are given in Sec. III D.

$$(E_1^{Cl} - E_3^{Cl}) = (E_1^K - E_3^K), \tag{3}$$

$$10(E_0^{Cl} - E_3^{Cl}) = 5(E_0^K - E_2^K) - 3(E_1^K - E_2^K) - 17(E_3^K - E_2^K), \tag{4}$$

where the superscript designates the nucleus and the subscript the spin of the level. With the experimental excitation energies of the $(\pi 1d_{3/2})(\nu 1f_{7/2})$ and $(\pi 1d_{3/2})(\nu 2p_{3/2})$ quadruplets in K^{40} taken from Ref. 34, the Pandya transformation gives for Cl^{38} the results shown in Fig. 13. The relative position of the two quadruplets is arbitrary, as the Pandya transformation relates only energy-level differences for a given multiplet.

The excellent agreement with the experimentally observed level scheme is well known[7] for the $(\pi 1d_{3/2})(\nu 1f_{7/2})$ quadruplet. With respect to the $(\pi 1d_{3/2})(\nu 2p_{3/2})$ quadruplet, the suggestion of spins 1^-, 0^-, and 2^- for levels at 1692, 1746, and 1981 keV, respectively, is in agreement with the experimentally allowed spin assignments and is also supported by the observed $l=1$ strength for these levels in the (d, p) reaction.[1,3] It would be of interest to obtain experimentally unique spin assignments to further test these suggestions.

D. Shell-Model Calculations

Shell-model calculations which describe negative-parity states in nuclei in the upper end of the (s, d) shell are scarce, and are generally performed in a limited configuration space[5,6,38] so that only a first-order picture emerges. Results for Cl^{38} are shown in Fig. 14.

In calculation (a), configurations of the form $(1d_{3/2})^{-3}(1f_{7/2})$ are considered[5] and the $f_{7/2}$ quadruplet in Cl^{38} is well reproduced, indicating that this is probably the dominant configuration.

In calculation (b) this model is extended[6] by allowing excitations from the $1d_{3/2}$ shell, to both the $1f_{7/2}$ and $2p_{3/2}$ shell, to account, e.g., for some of the $l_n=1$ stripping strength observed in the (d, p) reaction. From the results shown in Fig. 14 it can be seen that: (1) the $2p_{3/2}$-$1f_{7/2}$ single-particle energy splitting, which was taken from Ca^{41} and Sc^{41} and kept fixed at 1.93 MeV in the calculation, is too large; and (2) the members of the $(1d_{3/2})^{-3}(2p_{3/2})$ quadruplet are spread out too much, indicating admixtures from other configurations.

Spectrum (c) in Fig. 14 is the preliminary result[9] of a shell-model calculation involving a larger configuration space. Configurations of the form $(1d_{5/2}, 2s_{1/2})^{-n}(1d_{3/2})^{1+n}(\rho)$ with respect to a $_{16}S_{20}^{36}$ core were taken into account. The symbol ρ denotes a neutron in the $1f_{7/2}$, $2p_{3/2}$, or $1f_{5/2}$ shell, and the number of proton holes in the $(1d_{5/2}, 2s_{1/2})$ shell is restriced to $n=0$ or 1. Single-particle energies are deduced from neighboring nuclei and the calculation makes use of bare Kuo-

Brown matrix elements.

ACKNOWLEDGMENTS

We would like to thank P. Goode for permission to quote results of his calculations prior to publication and C. E. Regan, III, for the use of his Doppler program FTAU. We would like to thank C. Z. Nawrocki for making the $BaCl_2^{37}$ targets.

---

†Work supported under the auspices of the U. S. Atomic Energy Commission.

[1]J. Rapaport and W. W. Buechner, Nucl. Phys. 83, 80 (1966).

[2]C. H. Paris, W. W. Buechner, and P. M. Endt, Phys. Rev. 100, 1317 (1955).

[3]A. M. Hoogenboom, E. Kashy, and W. W. Buechner, Phys. Rev. 128, 305 (1962).

[4]R. E. Segel, G. H. Wedberg, G. B. Beard, N. G. Puttaswamy, and N. Williams, Phys. Rev. Letters 25, 1352 (1970).

[5]F. C. Erné, Nucl. Phys. 84, 91 (1966).

[6]G. A. P. Engelbertink and P. W. M. Glaudemans, Nucl. Phys. A123, 225 (1969).

[7]S. P. Pandya, Phys. Rev. 103, 956 (1956); S. Goldstein and I. Talmi, *ibid.* 102, 589 (1956).

[8]J. A. Becker and E. K. Warburton, Phys. Rev. Letters 26, 143 (1971).

[9]P. Goode, University of Rochester, private communication.

[10]G. A. P. Engelbertink, H. Lindeman, and M. J. N. Jacobs, Nucl. Phys. A107, 305 (1968).

[11]J. van Klinken, F. Pleiter, and H. T. Dijkstra, Nucl. Phys. A112, 372 (1968).

[12]J. B. Marion, Nucl. Data A4, 301 (1968).

[13]R. C. Greenwood, R. G. Helmer, and R. J. Gehrke, Nucl. Instr. Methods 77, 141 (1970).

[14]G. A. P. Engelbertink and J. W. Olness, Phys. Rev. C 3, 180 (1971).

[15]P. M. Endt and C. van der Leun, Nucl. Phys. A105, 1 (1967).

[16]A. H. Wapstra, G. J. Nijgh, and R. van Lieshout, *Nuclear Spectroscopy Tables* (North-Holland, Amsterdam, 1959).

[17]I. S. Towner, University of Oxford, private communication.

[18]S. I. Baker and R. E. Segel, Phys. Rev. 170, 1046 (1968).

[19]G. A. P. Engelbertink and G. van Middelkoop, Nucl. Phys. A138, 588 (1969).

[20]W. M. Currie, L. G. Earwaker, and J. Martin, Nucl. Phys. A135, 325 (1969).

[21]T. Holtebekk, R. Strømme, and S. Tryti, Nucl. Phys. A142, 251 (1970).

[22]K. S. Burton and L. C. McIntyre, Jr., Nucl. Phys. A154, 551 (1970).

[23]J. Lindhard, M. Scharff, and H. E. Schiøtt, Kgl. Danske Videnskab. Selskab, Mat.-Fys. Medd. 33, No. 14 (1963).

[24]A. E. Blaugrund, Nucl. Phys. 88, 501 (1966).

[25]J. H. Ormrod, J. R. MacDonald, and H. E. Duckworth, Can. J. Phys. 43, 275 (1965).

[26]B. Fastrup, P. Hvelplund, and C. A. Sautter, Kgl. Danske Videnskab. Selskab, Mat.-Fys. Medd. 35, No. 10 (1966).

[27]P. Hvelplund and B. Fastrup, Phys. Rev. 165, 408 (1968).

[28]E. K. Warburton, J. W. Olness, G. A. P. Engelbertink, and T. K. Alexander, to be published.

[29]J. W. Olness and E. K. Warburton, Phys. Rev. 151, 792 (1966).

[30]E. K. Warburton, J. W. Olness, and A. R. Poletti, Phys. Rev. 160, 938 (1967).

[31]R. E. Segel, in *Proceedings of the Fourth International Symposium on Light Medium Mass Nuclei* (University of of Kansas Press, Lawrence, Kansas, 1970).

[32]P. Kienle, K. Wien, F. Wunderlich, and R. Haas, Z. Physik 170, 76 (1962).

[33]B. Bošnjaković, J. A. van Best, and J. Bouwmeester, Nucl. Phys. A94, 625 (1967).

[34]R. M. Freeman and A. Gallman, Nucl. Phys. A156, 305 (1970).

[35]J. C. Hardy, H. Brunnader, and J. Cerny, Phys. Rev. C 1, 561 (1970).

[36]H. Brunnader, Ph.D. thesis, Lawrence Radiation Laboratory, University of California, 1969 (unpublished).

[37]S. Maripuu, Nucl. Phys. A123, 357 (1969).

[38]S. Maripuu and G. A. Hokken, Nucl. Phys. A141, 481 (1970).